We are IntechOpen, the world's leading publisher of Open Access books Built by scientists, for scientists

4,800
Open access books available

122,000
International authors and editors

135M
Downloads

Our authors are among the

154
Countries delivered to

TOP 1%
most cited scientists

12.2%
Contributors from top 500 universities

CLARIVATE ANALYTICS BOOK CITATION INDEX INDEXED

WEB OF SCIENCE™

Selection of our books indexed in the Book Citation Index in Web of Science™ Core Collection (BKCI)

Interested in publishing with us?
Contact book.department@intechopen.com

Numbers displayed above are based on latest data collected.
For more information visit www.intechopen.com

6

Tissue Harmonic Imaging with Coded Excitation

Masayuki Tanabe[1,2], Takuya Yamamura[2], Kan Okubo[2] and Norio Tagawa[2]
[1]*JSPS Research Fellow*
[2]*Graduate School of System Design, Tokyo Metropolitan University*
Japan

1. Introduction

It becomes more important to obtain medical ultrasound images with higher signal-to-noise ratio (SNR) and higher spatial resolution. In the last decade, tissue harmonic imaging (THI) and coded excitation to medical ultrasound imaging have been investigated. Coded excitation can overcome the trade-off between spatial resolution and penetration, which occurs when using the conventional pulse (Chiao, 2005), (Hu et al., 2001), (Tanabe et al., 2008). It is said that chirp signal is the most robust code for medical ultrasound image (Misaridis & Jensen, 2005). THI can acquire higher spatial resolution image and has been used in the commercial medical ultrasound system. A combination of coded excitation and THI (coded THI) has been investigated (Arshadi et al., 2007), (Hu et al., 2001), (Song et al., 2010), (Tanabe et al., 2010).
As a problem of THI, the frequency bandwidths of the fundamental and the harmonic components often overlap. The spectral overlap causes degradation of spatial resolution and the undesirable artifact. For the solution to the problem, only the harmonic component is extracted by pulse inversion (PI) method. However, if reflectors in the region of interest (ROI) move even a little, the fundamental components of echos are not cancelled completely. The intensity of the extracted harmonic components is still much smaller than the intensity of the residual fundamental component. Hence, the residual fundamental component has a bad effect on THI.
In sections II through IV, THI, coded excitation, and the combination of them are explained. In section V, we propose a new method which can extract broader bandwidth of the harmonic component for coded THI. The feasibility of the method is evaluated with experiments and simulations, and the expected performance in term of axial resolution and SNR has been verified.

2. Tissue harmonic imaging

THI has become a more common option for B-mode scanning. THI makes use of the nonlinearity of the sound propagation in the medium. The equation of a sound velocity c is expressed as

$$c = c_0 + \frac{1}{\rho_0 c_0}\left(\frac{B}{2A} + 1\right)p, \tag{1}$$

where c_0 is a sound velocity at atmospheric pressure, ρ_0 is an atmospheric density, B/A is a nonlinear parameter, and p is a sound pressure. The sound velocity increases at high acoustic pressures, and decreases at negative high acoustic pressures, and thus, the signal is distorted, as shown in Fig. 1(a). The harmonic components generate gradually, so that THI can obtain further region of interest. Additionally, The beamwidth of the harmonic component is narrower than that of the fundamental component. Therefore, THI can suppress sidelobe artifacts. However, there is frequency dependent attenuation (FDA) in human body, thus, the harmonic components attenuate more greatly than the fundamental components. Therefore, it is said that the intensity of the harmonic component depends on the propagation distance and the excitation intensity.
The amplitude of the harmonic component is much smaller than that of the fundamental component, thus, THI suffers from the poor SNR, resulting in limited penetrating depth.

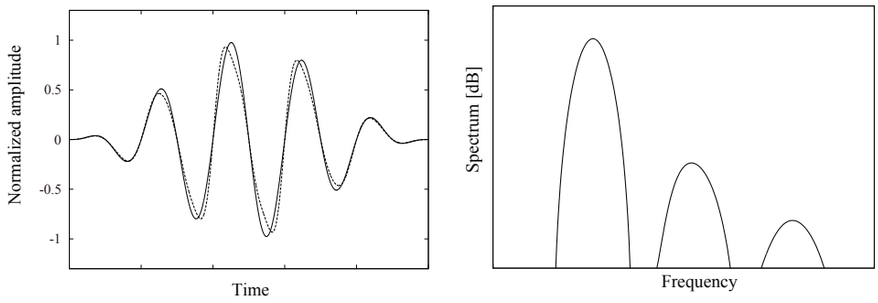

(a) (b)

Fig. 1. THI. (a) Initial signal (solid line) and distorted signal (dash line). (b) Frequency spectrum of distorted signal.

3. Coded excitation

Next, let me explain coded excitation with linear chirp signal. The linear chirp signal is defined as a signal which frequency changes linearly, as described below

$$s(t) = \sin[2\pi(f_0 + \frac{B}{2T}t)t], \text{ for } 0 \leq t \leq T, \tag{2}$$

where f_0 is a starting frequency, B is a frequency bandwidth, and T is a time duration. An example of the linear chirp signal and its frequency spectrum are shown in Figs. 2 (b) and 2 (c). To decode the signal, auto-correlation function (ACF) is calculated as

$$\text{ACF}(\tau) \quad = \quad \int_{-\infty}^{\infty} s(t)s(t-\tau)dt, \tag{3}$$

where τ is a time shift. The ACF and its envelope are shown in Fig. 2(d). The half-bandwidth of the decoded signal is $1/B$ [s]. The SNR improvement is determined by the product of the duration T [s] and the bandwidth B [Hz] of the signal; it is called time-bandwidth product (TBP). An unmodulated pulse of duration T [s] at a carrier frequency f_c $(= f_0 + B/2)$ [Hz] has a frequency bandwidth $B = 1/T$ [Hz] around f_c [Hz]. The SNR of the decoded signal is

TB times higher than the unmodulated pulse. An advantage of chirp signal is to design the frequency bandwidth within the system properties.

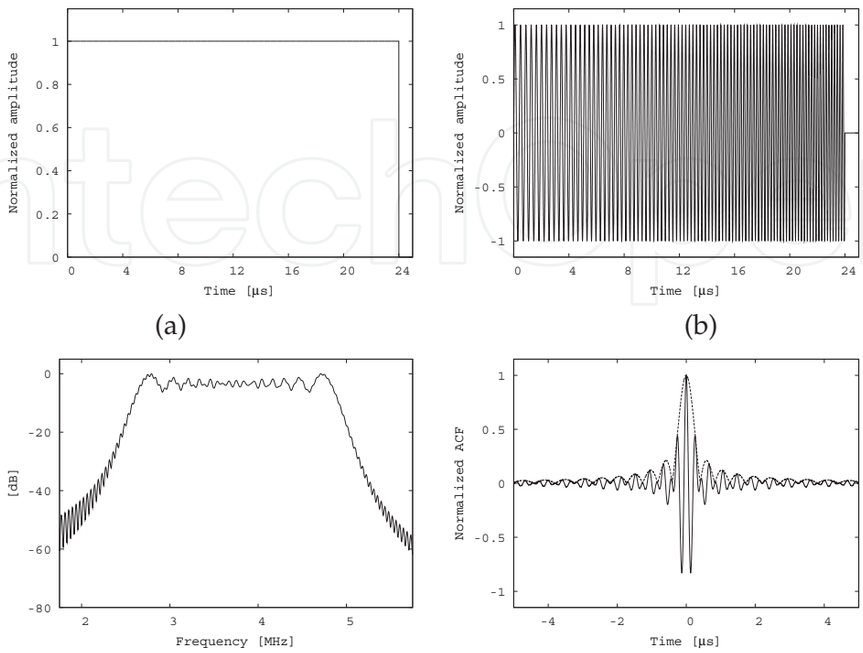

Fig. 2. Chirp signal with rectangular window. Time duration is 24 μs, and frequency is 2.5−5 MHz. (a) Window shape, (b) time domain, (c) frequency spectrum, and (d) ACF (solid line) and its envelope (dashed line).

As shown in Fig. 2(d), the rectangular window causes a range sidelobe. The range sidelobe has a bad effect on imaging. For suppression of the sidelobe, the signal is weighted by a window function. For example, the Hanning window $w_1(t)$ is expressed as

$$w_1(t) = 0.5 - 0.5\cos(2\pi t/T) \text{ for } 0 \leq t \leq T. \tag{4}$$

Figure 3 describes a Hanning weighted chirp signal. As shown in Fig. 3(d), the ACF of the Hanning window doesn't cause a range sidelobe. However, the half pulse-width is wider than that of the rectangular window as shown in Figs. 2(d) and 3(d).
It is said that there is a trade-off between the range sidelobe level and the half pulse-width. As a derived form of the Hanning window, the Hanning window is applied at starting and ending parts of the signal below

$$w_2(t) = \begin{cases} 0.5 - 0.5\cos(\pi t/(dT)) & (0 \leq t \leq dT) \\ 1 & (dT \leq t \leq (1-d)T) \\ 0.5 - 0.5\cos(\pi(t-T)/(dT)) & ((1-d)T \leq t \leq T), \end{cases} \tag{5}$$

where, d is the starting and the ending ratio. Figure 4 describes a chirp signal with the window in which d is 0.3.

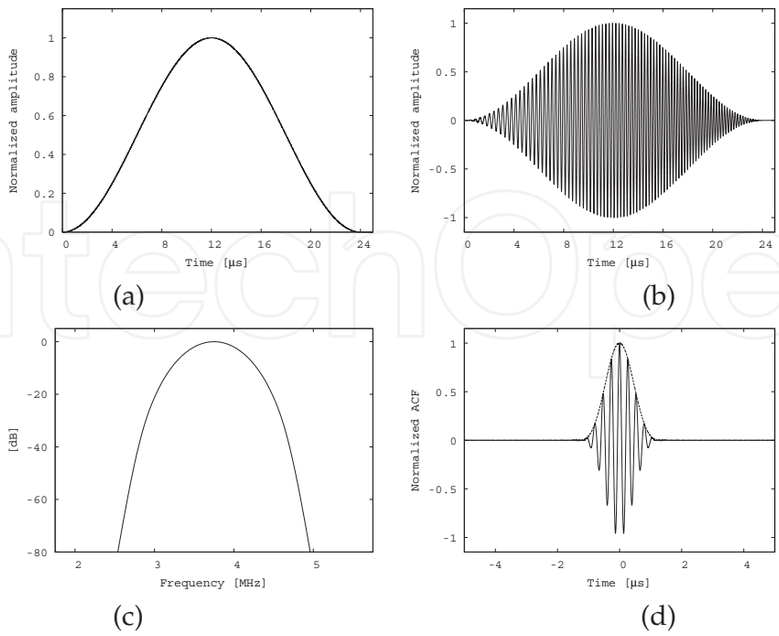

Fig. 3. Chirp signal with Hanning window. Time duration is 24 μs, and frequency is 2.5−5 MHz. (a) Window shape, (b) time domain, (c) frequency spectrum, and (d) ACF (solid line) and its envelope (dashed line).

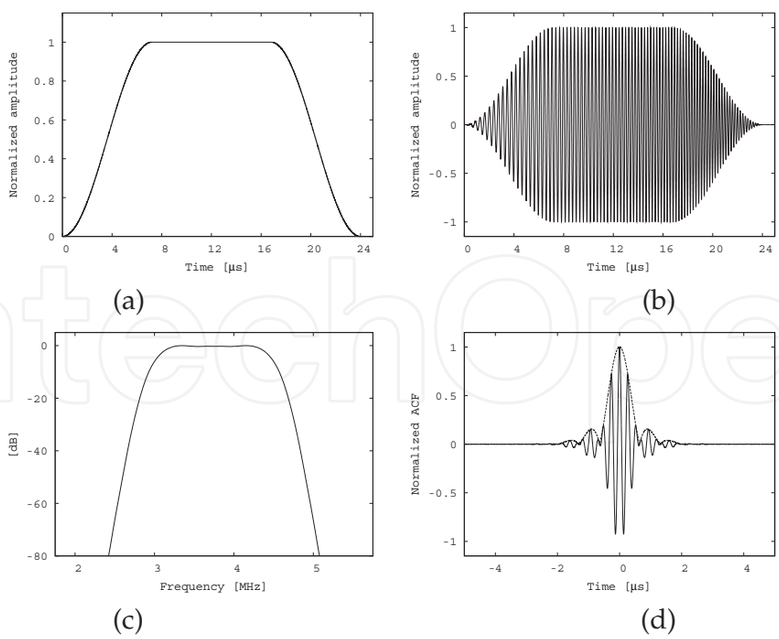

Fig. 4. Chirp signal with partial Hanning window (d=0.3). Time duration is 24 μs, and frequency is 2.5−5 MHz. (a) Window shape, (b) time domain, (c) frequency spectrum, and (d) ACF (solid line) and its envelope (dashed line).

The window shapes and the ACFs with various d are shown in Figs. 5(a) and 5(b).

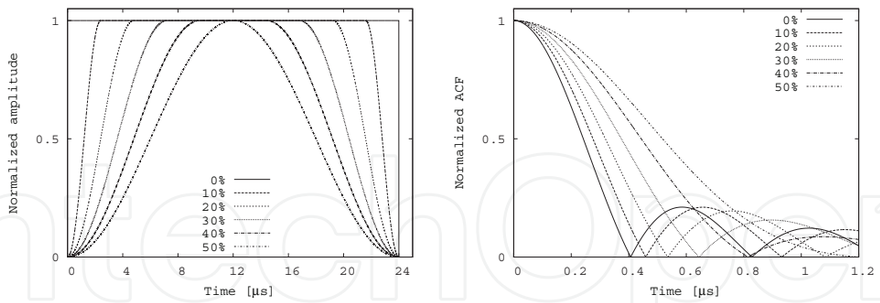

(a) (b)

Fig. 5. (a) Window shapes and (b) envelopes of ACFs with various d. Time duration is 24 μs, and frequency is 2.5−5 MHz.

It is said that the window shape has an influence on the spatial resolution and the sidelobe level and that there is a trade-off between the spatial resolution and the sidelobe level.
In actual use, after transmission of $s(t)$, an echo signal $r(t)$ is received. To decode the signal, the cross-correlation function (CCF) is calculated as

$$\mathrm{CCF}(\tau) = \int_0^\infty r(t)s(t-\tau)dt. \tag{6}$$

4. Coded tissue harmonic imaging and spectral overlap consideration

To obtain both sufficient SNR and spatial resolution, a method which combines THI and coded excitation, has been proposed. When a chirp signal is transmitted into the medium, the obtained echo has harmonic components. The harmonic component of the chirp is also chirp because chirp maintains their coded phase relationship in the harmonic domain (Misaridis & Jensen, 2005). Therefore, the harmonic component can be compressed with a matched filter. The template signal used in the matched filter for the harmonic component is designed as the same time duration, and twice as bandwidth as the fundamental component of the chirp as

$$m(t) = \sin[2\pi(2f_0 + \frac{B}{T}t)t]. \text{ for } 0 \le t \le T \tag{7}$$

If the harmonic and the fundamental components are not overlapped in frequency domain, the harmonic component can be isolated by bandpass filtering (BF) as shown in Fig. 6(a). However, if the harmonic component overlaps the fundamental component in frequency domain due to the frequency broadness of the transmitted signal, the overlapped part of the harmonic component cannot be extracted. Therefore, in the BF, the extracted bandwidth has to be narrower, and thus, the image quality becomes poor, as shown in Fig. 6(b).
For avoiding the spectral overlap in THI, pulse inversion (PI) method has been used. The PI transmits two phase-inverted pulses, as shown in Fig. 7. By simply summing two echo signals, the harmonic component is doubled, and the fundamental component is cancelled, as shown in Fig. 8. However, if the PI is used for fast moving target such as cardiac valves, phase decorrelation occurs and the cancellation of the fundamental component cannot be done.

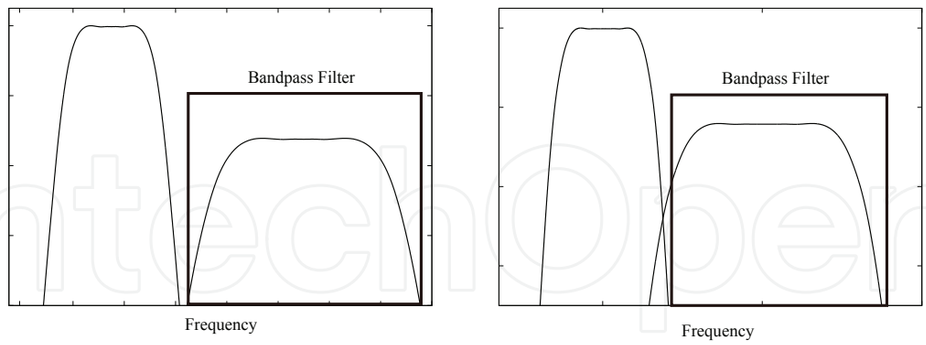

(a) (b)

Fig. 6. Bandpass filter (a) when overlap doesn't occur and (b) occurs.

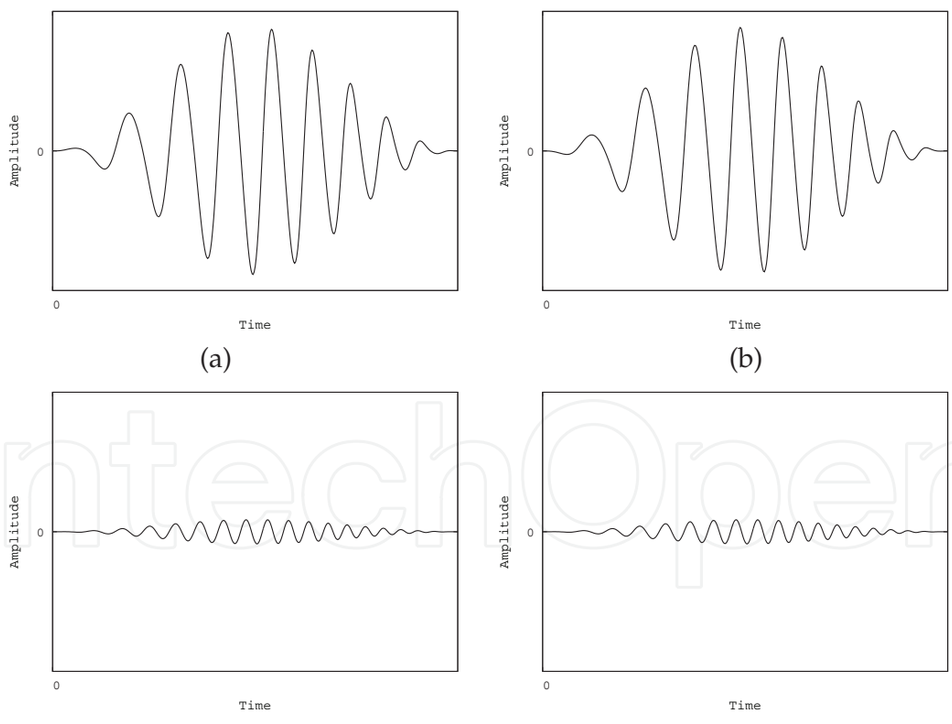

(a) (b)

(c) (d)

Fig. 7. (a) (b) Transmitted signals of pulse inversion and (c) (d) harmonic components of received signals.

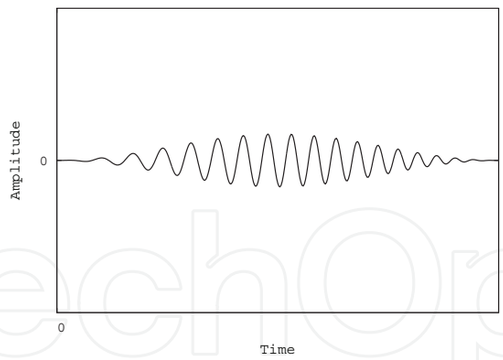

Fig. 8. Sum of received signals of pulse inversion.

In coded THI, there still remains the problem of the spectral overlap, which exists in THI. The matched filter is designed for the harmonic component. There is a cross-correlation between the fundamental frequencies of received echo and the second harmonic matched filter. As a result, an undesirable peak occurs at different time from the time of arrival.
By suppressing the bandwidth to avoid the spectral overlap, the problem does not occur as shown in Fig. 6(b), but the spatial resolution becomes worse. As mentioned above, we can of course also apply the PI, but the method is susceptible to the target motion.
In this study, a novel harmonic isolation method is proposed, and the impact of spectral overlap is examined through simulations and experiments.

5. Method

5.1 Principle

In this section, we explain the proposed method. The method uses multi chirp signals. The spectrum of the each signal is designed for not overlapping between the fundamental and harmonic components. The each chirp signal is transmitted separately, and only the harmonic component of the echo signal can be extracted by the bandpass filter simply. Consequently, decoding with the isolated harmonic components, high spatial resolution signal with high SNR can be obtained.

5.2 Coding process

When the number of excitations is defined as N, the i^{th} chirp signal $s_i(t)$ $(i = 1, 2, ..., N)$ is expressed as

$$s_i(t) = \alpha(t) \sin\{2\pi[f_i + \frac{B}{2T} \cdot t] \cdot t\}, \quad (0 \leq t \leq T/N), \tag{8}$$

$$f_i = f_0 + \frac{B(i-1)}{N}, \tag{9}$$

where $\alpha(t)$ is the amplitude modulation, f_i is the i^{th} starting frequency, B/N is the bandwidth of each shot, T/N is the time duration of each shot.

5.3 Matched filter and decoding process

After transmission, N echo signals are received. The harmonic component of the each echo signal is separated from the fundamental component. Therefore, it is easy to isolate the harmonic component by bandpass filtering.

For decoding with the harmonic components, the each matched filter $m_i(t)$ has a same time duration and a twice frequency bandwidth as the transmitted signal.

$$m_i(t) = \alpha(t) \sin 2\pi[2f_i + \frac{B}{T}t]t, \quad (0 \leq t \leq T/N). \tag{10}$$

The echo signals $r_i(t)_{i=1,2,\ldots,N}$ are decoded bellow

$$CCF(\tau) = \sum_{i=1}^{N}[\int_0^{\infty} r_i(t)m_i(t-\tau)dt]. \tag{11}$$

The TBP of the decoded signal is assumed as TB below

$$(T/N \times N) \times (B/N \times N) = TB. \tag{12}$$

6. Experiments and simulations

6.1 Experimental procedure

To evaluate the proposed method, *in vitro* experiments are conducted. The stainless steel block is placed in a water tank. The signal is transmitted by a transducer (KB-AEROTECH MLB50DL, the center frequency is 5 MHz). Figure 9 describes the experimental circumstance. In the proposed method, N is 2, the frequencies of the proposal are 2.5−3.7 MHz and 3.6−5 MHz, the time duration 13.5 μs, each 3 μs of the start and the end of the signal is half of the Hanning window ($d = 3/13.5$)..

For comparison, conventional coded THI method is also used. The frequency of the conventional type is 2.5−5 MHz, time duration 24 μs, and each 3 μs of start and end of the signal is half of the Hanning window ($d = 0.125$). The time duration of conventional coded THI is adjusted as sum of two signals of the proposed method. Figures 10, 11(a) and (b) describe the transmitted signals.

6.2 Axial resolution

The received echo signals are shown in Figs. 12(a), 13(a) and 13(b). As shown in Fig. 12(b), in conventional coded THI, the harmonic component is overlapped with the fundamental component at −30 dB. While, as shown in Fig. 14, in proposal, the each harmonic component is overlapped with the fundamental component at approximately −55 dB and −60 dB. Therefore, it is obvious that the proposed method can obtain the harmonic component more easily than the conventional method.

Subsequently, envelopes of the CCFs are shown in Figs. 15 and 16. In Figs. 15 and 16, the solid and the dashed lines describe the CCF using the fundamental and the harmonic components, respectively. Fig. 15 (b) is a part at 86−90 μs of Fig. 15(a). As shown in Fig. 15(b), it is shown that the CCF of the harmonic component is narrower than that of the fundamental component. However, in conventional coded THI, it is shown that the CCF with the harmonic component has an artifact at approximately 110 μs, as shown in Fig. 15(a). The artifact is the

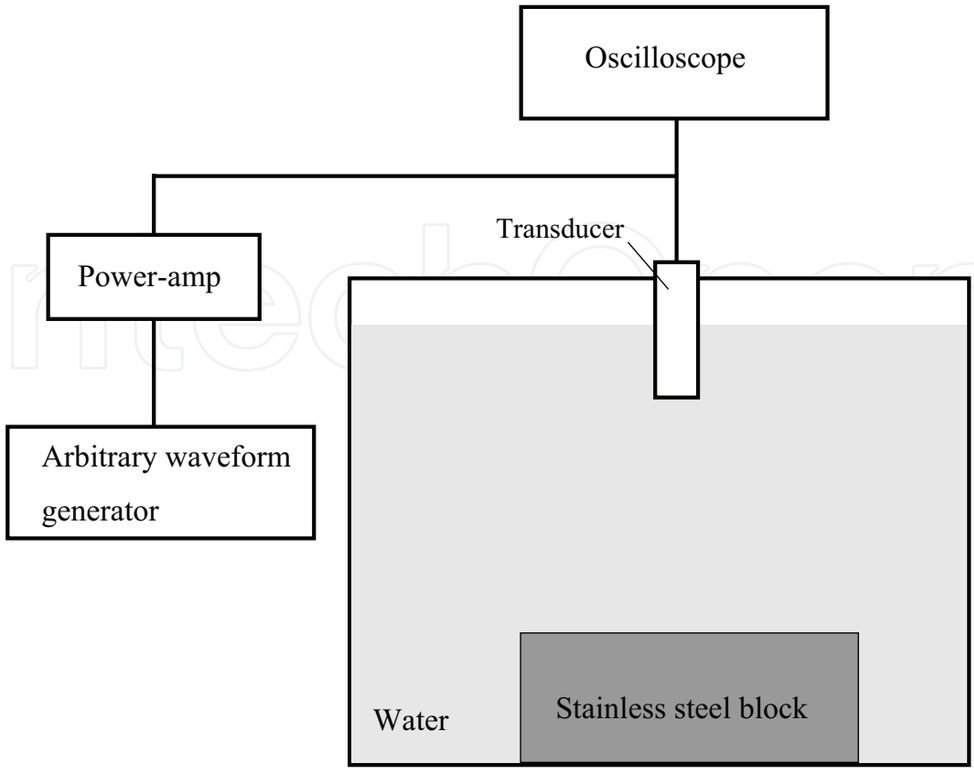

Fig. 9. Experimental circumstance

cross-correlation between the fundamental component of the echo signal and the harmonic matched filter. The CCF of the proposal, there is no artifact such as the conventional THI, and the CCFs of the fundamental and the harmonic components have the same axial resolution as that of the conventional THI.

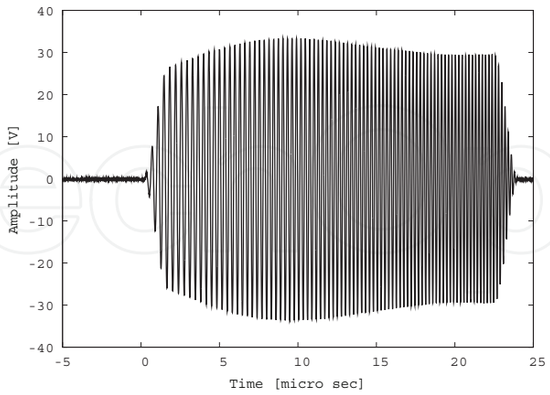

Fig. 10. Transmitted signal of conventional coded THI.

6.3 SNR

To examine the SNR of the proposed method, the decibel representations of the envelopes of the CCFs in conventional coded THI are shown in Figs. 17(a) and (b), and those of

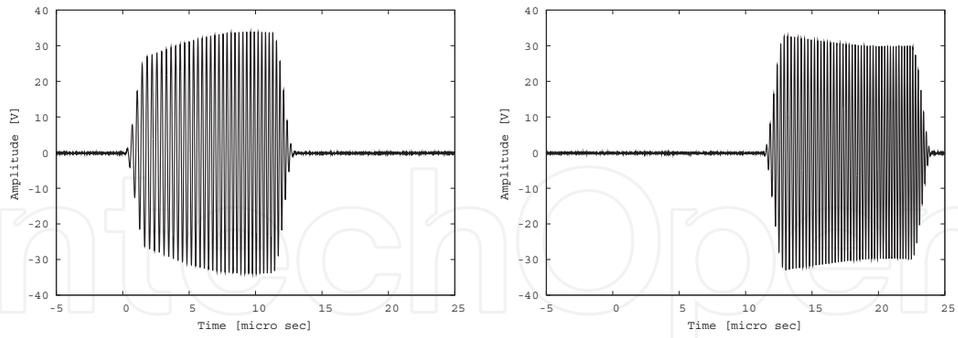

(a) (b)

Fig. 11. Transmitted signals of proposed coded THI. (a)1st and (b)2nd shots.

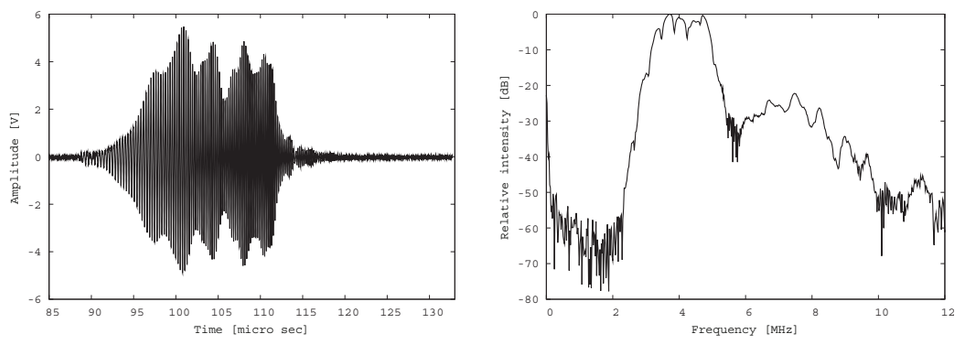

(a) (b)

Fig. 12. Echo signal of conventional coded THI in (a)time domain and (b)frequency domain.

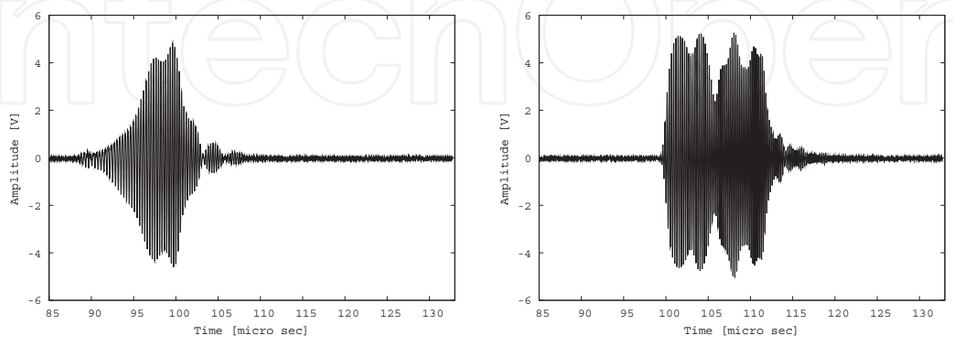

(a) (b)

Fig. 13. Echo signals of proposed coded THI in time domain. (a)1st and (b)2nd shots.

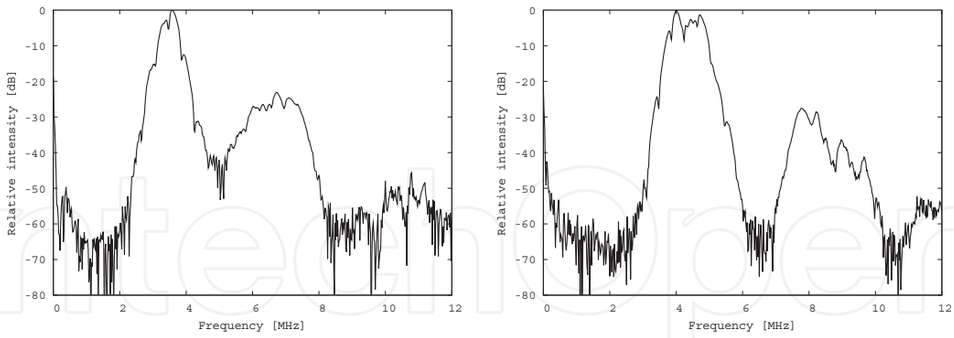

(a) (b)

Fig. 14. Echo signals of proposed coded THI in frequency domain. (a)1st and (b)2nd shots.

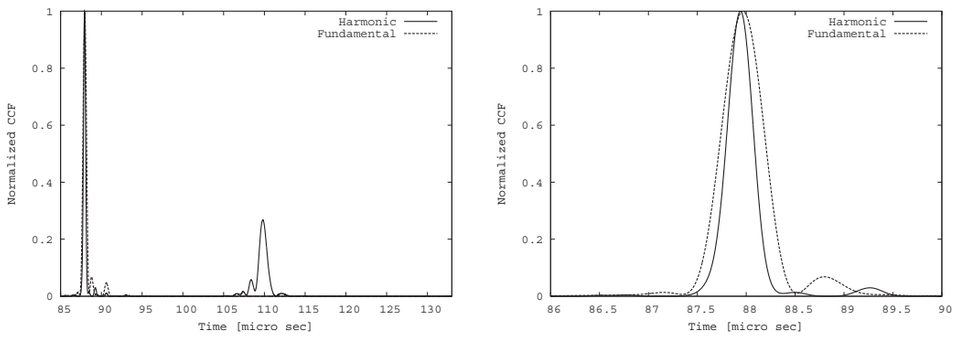

(a) (b)

Fig. 15. Envelope of CCF of conventional coded THI at (a)85-135 μs and (b)86-90 μs.

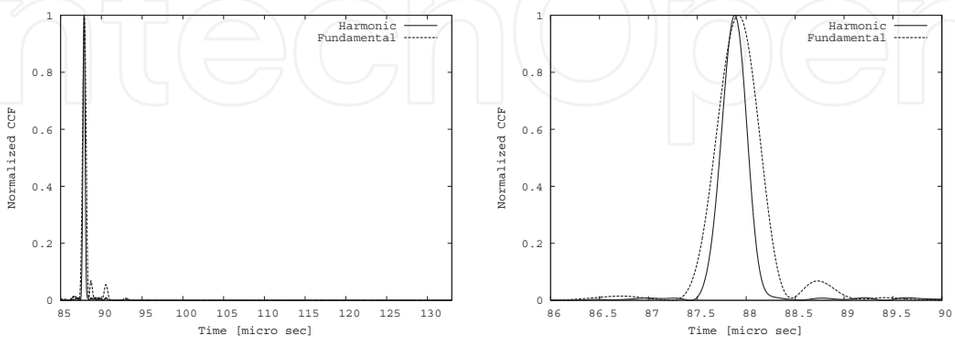

(a) (b)

Fig. 16. Envelope of CCF of proposed coded THI at (a)85-135 μs and (b)86-90 μs.

proposed method are shown in Figs. 18(a) and (b). As compared with conventional coded THI, excepting the artifact at approximately 110 μs, it is shown that the proposed method can obtain almost the same SNR.

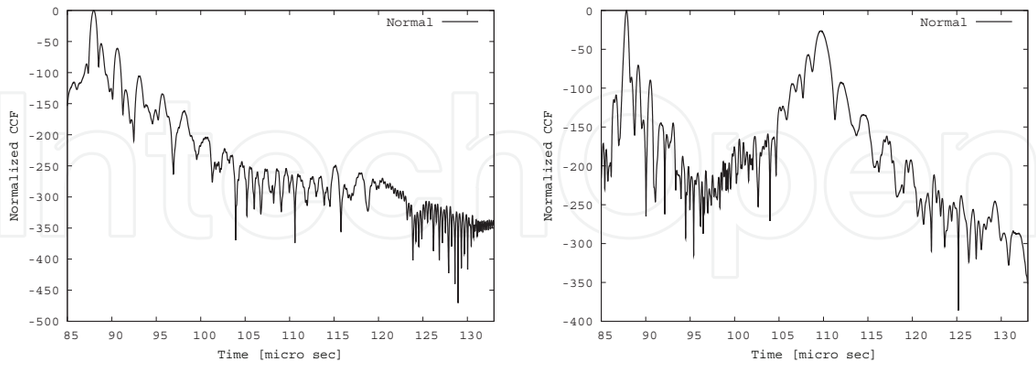

(a) (b)

Fig. 17. SNR of conventional coded THI. CCF with (a)fundamental and (b)harmonic components.

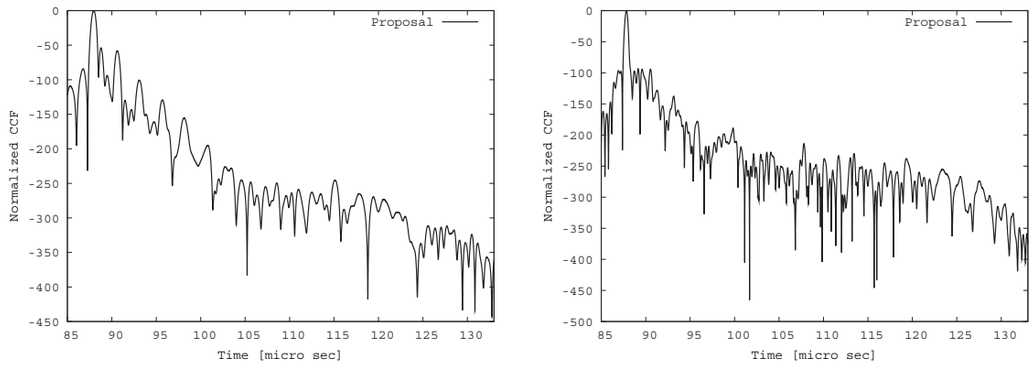

(a) (b)

Fig. 18. SNR of proposed coded THI. CCF with (a)fundamental and (b)harmonic components.

6.4 Tissue motion effects

The robustness of the proposal method against tissue motion is evaluated through FEM simulator PZFlex (Weidlinger Associates, Inc.). In a water tank, a point sound source is excited, and monitored from 6 cm away. In proposal, the number of shots N is 2, the each time duration is 20 μs, and the each frequency is $2-3.8$, and $3.2-5$ MHz, separately. For comparison, the pulse inversion method is also evaluated. In the PI method, the each transmitted signal is $2-5$ MHz and 20 μs. Time difference ξ between two shots is caused by tissue motion. In this study, the Doppler shift is ignored, and the time difference ξ is given as time shift artificially.

The received signals are shown in Figs. 19 and 20. When ξ=0 μs, as shown in Figs. 21(a),the fundamental components are cancelled completely, and the CCF can be conducted,

as shown in Figs. 21(a) and (b). When ξ=0.05 μs, as shown in Figs. 22(a), the fundamental components are not cancelled and and the spectral overlap occurs. As described in Fig. 22(b), the cross-correlation between the fundamental component and the harmonic matched filter occurs.
Figured 23 and 24 show the results of the proposed method. When ξ=0 μs, as shown in Fig. 23(b), the half pulse-width is the same as that of the PI. When ξ=0.05 μs, as shown in Fig. 24(b), the half-width of CCF is wider than that when ξ=0 μs, however, the cross-correlation like the PI does not occur.

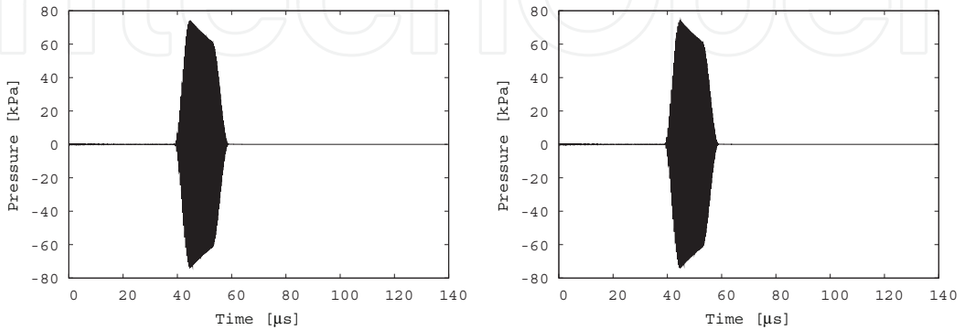

Fig. 19. Received signals of conventional coded THI with PI. (a)1st and (b)2nd shots.

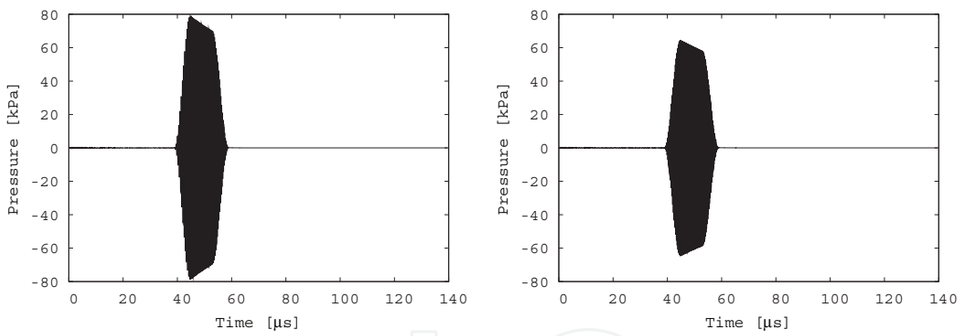

Fig. 20. Received signals of proposed coded THI. (a)1st and (b)2nd shots.

7. Conclusion

In this study, we proposed a new method which can avoid the occurrence of the spectral overlap. From the experimental results, it was shown that the proposed method can extract harmonic component. In simulations, it was shown that the proposed method can suppress the tissue motion effects compared with the PI.
This study is assumed that the imaging target has the static aspect. Although the Doppler shift was ignored in this study, the proposed method is still valid if the target moves at the constant speed. In future work, we will consider a situation that the target moves at an accelerating pace.

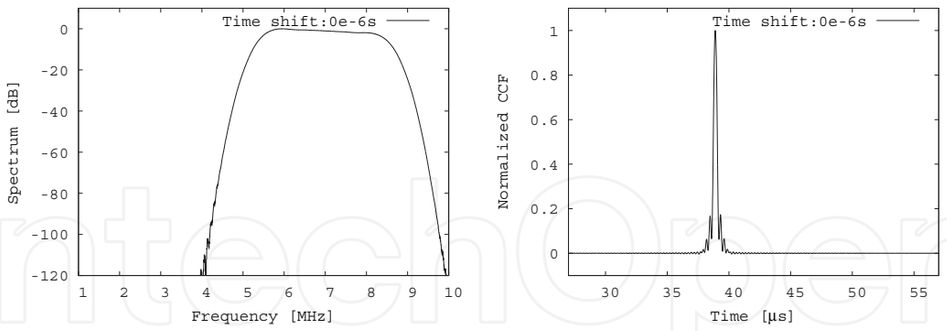

(a) (b)

Fig. 21. Received signals of conventional coded THI with PI when $\xi = 0\mu$s. (a) Frequency spectrum and (b) CCF.

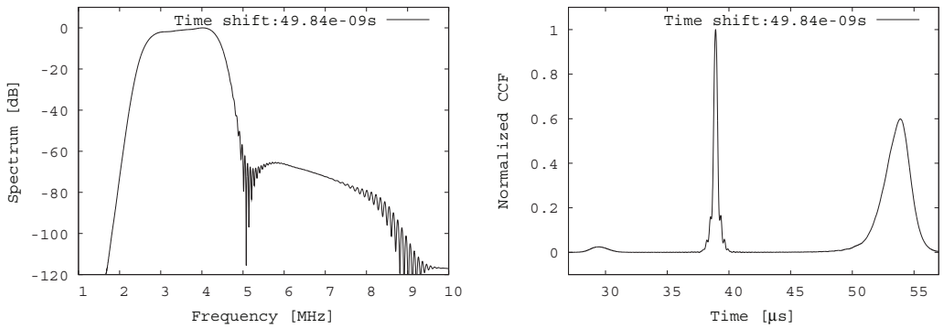

(a) (b)

Fig. 22. Received signals of conventional coded THI with PI when $\xi = 0.05\mu$s. (a) Frequency spectrum and (b) CCF.

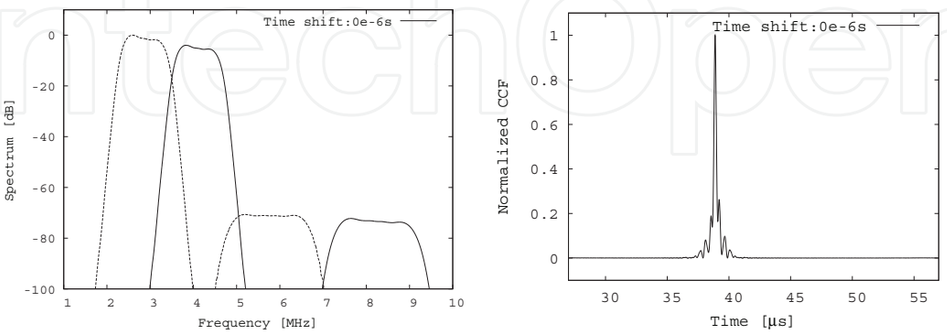

(a) (b)

Fig. 23. Received signals of proposed coded THI when $\xi = 0\mu$s. (a) Frequency spectrum and (b) CCF.

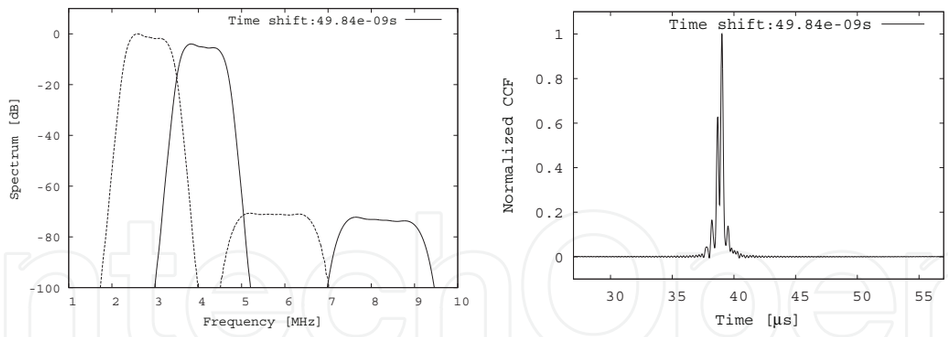

(a) (b)

Fig. 24. Received signals of proposed coded THI when $\xi = 0.05\mu$s. (a) Frequency spectrum and (b) CCF.

8. Acknowledgment

This work was partially supported by Grants-in-Aid for Scientific Research (B) (21300191) and Japan Society for the Promotion of Science.

9. References

Arshadi, R., Yu, A. C. H., & Cobbold, R. S. C. (2007). Coded Excitation Methods for Ultrasound Harmonic Imaging, *Canadian Acoustics*, Vol. 35 (No. 2), pp.35-46

Chiao, R. Y. & Hao X. (2005). Coded Excitation for Diagnostic Ultrasound: A System Developer's Perspective, *IEEE Transactions on Ultrasonics, Ferroelectrics and Frequency Control*, Vol. 52, pp.160-170

Hu, Z., Moriya, T., & Tanahashi, Y. (2001). Imaging System for Intravascular Ultrasonography Using Pulse Compression Technique, *Japanese Journal of Applied Physics*, Vol. 40, pp.3896

Kim, D. Y., Lee, J. C., Kwon, S. J., Song & T. K. (2001). Ultrasound Second Harmonic Imaging with a Weighted Chirp Signal, *Proceedings of IEEE Ultrasonics Symposium*, Atlanta, pp.1477-1480

Li, Y & Zagzebski, J. A. (2000). Computer Model for Harmonic Ultrasound Imaging, *IEEE Transactions on Ultrasonics, Ferroelectrics and Frequency Control*, Vol. 47 (No. 50), pp.1259-1272

Misaridis, T. & Jensen, J. A. (2005). Use of Modulated Excitation Signals in Medical UIltrasound. *IEEE Transactions on Ultrasonics, Ferroelectrics and Frequency Control*, Vol. 52, pp.177-219

Song, J., Kim, S., Sohn, H., Song & T., Yoo, Y. M. (2010). Coded Excitation for Ultrasound Tissue Harmonic Imaging, *Ultrasonics*, Vol. 50, pp.613-619

Tanabe, M., Okubo, K., Tagawa & N., Moriya, T. (2008). Inline Transmitter/Receiver System Using $Pb(Zn_{1/3}Nb_{2/3})O_3-PbTiO_3$ Single Crystal and Poly(Vinylidene Fluoride) for Harmonic Pulse Compression Imaging, *Japanese Journal of Applied Physics*, Vol. 47, pp.4149-4154

Tanabe, M., Yamamura, T., Okubo, K. & Tagawa, N. (2010). Medical Ultrasound Imaging Using Pulse Compression Technique Based on Split and Merge Strategy, *Japanese Journal of Applied Physics*, Vol. 49, pp.07HF15·1-07HF15·5

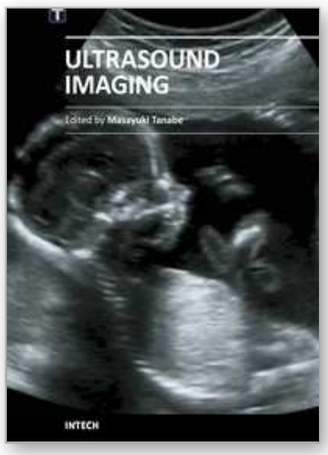

Ultrasound Imaging

Edited by Mr Masayuki Tanabe

ISBN 978-953-307-239-5
Hard cover, 210 pages
Publisher InTech
Published online 11, April, 2011
Published in print edition April, 2011

In this book, we present a dozen state of the art developments for ultrasound imaging, for example, hardware implementation, transducer, beamforming, signal processing, measurement of elasticity and diagnosis. The editors would like to thank all the chapter authors, who focused on the publication of this book.

How to reference

In order to correctly reference this scholarly work, feel free to copy and paste the following:

Masayuki Tanabe, Takuya Yamamura, Kan Okubo and Norio Tagawa (2011). Tissue Harmonic Imaging with Coded Excitation, Ultrasound Imaging, Mr Masayuki Tanabe (Ed.), ISBN: 978-953-307-239-5, InTech, Available from: http://www.intechopen.com/books/ultrasound-imaging/tissue-harmonic-imaging-with-coded-excitation

INTECH
open science | open minds

InTech Europe
University Campus STeP Ri
Slavka Krautzeka 83/A
51000 Rijeka, Croatia
Phone: +385 (51) 770 447
Fax: +385 (51) 686 166
www.intechopen.com

InTech China
Unit 405, Office Block, Hotel Equatorial Shanghai
No.65, Yan An Road (West), Shanghai, 200040, China
中国上海市延安西路65号上海国际贵都大饭店办公楼405单元
Phone: +86-21-62489820
Fax: +86-21-62489821

IntechOpen